NANO MICRO small
www.small-journal.com

Nanostructuring Lipophilic Dyes in Water Using Stable Vesicles, Quatsomes, as Scaffolds and Their Use as Probes for Bioimaging

Antonio Ardizzone, Siarhei Kurhuzenkau, Sílvia Illa-Tuset, Jordi Faraudo, Mykhailo Bondar, David Hagan, Eric W. Van Stryland, Anna Painelli, Cristina Sissa, Natalia Feiner, Lorenzo Albertazzi, Jaume Veciana, and Nora Ventosa**

A new kind of fluorescent organic nanoparticles (FONs) is obtained using quatsomes (QSs), a family of nanovesicles proposed as scaffolds for the nanostructuration of commercial lipophilic carbocyanines (1,1′-dioctadecyl-3,3,3′,3′-tetramethyl-indocarbocyanine perchlorate (DiI), 1,1′-dioctadecyl-3,3,3′,3′-tetramethyl-indodicarbocyanine perchlorate (DiD), and 1,1′-dioctadecyl-3,3,3′,3′-tetramethyl-indotricarbocyanine iodide (DiR)) in aqueous media. The obtained FONs, prepared by a CO_2-based technology, show excellent colloidal- and photostability, outperforming other nanoformulations of the dyes, and improve the optical properties of the fluorophores in water. Molecular dynamics simulations provide an atomistic picture of the disposition of the dyes within the membrane. The potential of QSs for biological imaging is demonstrated by performing superresolution microscopy of the DiI-loaded vesicles in vitro and in cells. Therefore, fluorescent QSs constitute an appealing nanomaterial for bioimaging applications.

Dr. A. Ardizzone, Dr. J. Faraudo, Prof. J. Veciana, Dr. N. Ventosa
Institut Ciencia Materials Barcelona (ICMAB-CSIC)-CIBER-BBN
Campus Universitari de Bellaterra
08193 Cerdanyola, Spain
E-mail: veciana@icmab.es; ventosa@icmab.es
Dr. S. Kurhuzenkau, Prof. A. Painelli, Dr. C. Sissa
Dipartimento di Scienze Chimiche, della Vita e della Sostenibilità Ambientale
Università di Parma
Parco Area Delle Scienze 17/A, 43124 Parma, Italy
S. Illa-Tuset
Theoretical Sciences Unit
JNCASR
Bangalore 560064, India
Prof. M. Bondar
Institute of Physics
National Academy of Sciences of Ukraine
Prospect Nauky 46, Kyiv 03028, Ukraine
Dr. D. Hagan, Prof. E. W. Van Stryland
The College of Optics and Photonics (CREOL)
University of Central Florida
P.O. Box 162700, Orlando, FL 32816-2700, USA
N. Feiner, Dr. L. Albertazzi
Institute for Bioengineering of Catalonia (IBEC)
Parc Cientìfic de Barcelona (PCB)
08028 Barcelona, Spain
The ORCID identification number(s) for the author(s) of this article can be found under https://doi.org/10.1002/smll.201703851.

DOI: 10.1002/smll.201703851

Fluorescent organic dyes are widely investigated as fluorescent probes in microscopy, thanks to their tunable optical and physicochemical properties via chemical modification of their structure.[1] Good fluorescent probes for microscopy should be bright and highly photostable; water soluble; and chemically stable in buffers, cell media, or body fluids; as well as capable of site-specific labeling and showing biocompatibility.[2] Small organic molecules can be highly fluorescent, although they may suffer poor solubility in aqueous media (particularly so for red and infrared dyes),[3] limiting their use for bioapplications.[4] Loading an organic dye into a nonfluorescent nanocarrier, arranged as fluorescent organic nanoparticle (FON), offers an interesting strategy to bring organic dyes in aqueous media, since the obtained FONs have in general good brightness, photostability, and biocompatibility.[5–9] These nanostructures also have well-known physicochemical properties and can be loaded or grafted with bioactive compounds and/or targeting agents, to produce multifunctional nanoparticles for theranostic applications.[10]

Small unilamellar vesicles (SUVs), e.g., liposomes, with sizes of ≈100 nm, are intensively investigated supramolecular nanostructures for such purposes.[11,12] Indeed, their membranes offer opportunities for an efficient functionalization and for this reason they find various biological applications, including drug delivery, labeling, and bioimaging.[11,13,14] In spite of extensive studies on SUVs, only a few works have been focused on their capability to nanostructure organic dyes.[15–17] Moreover, there is a strong interest toward new vesicular formulations, made by nonlipid components, able to overcome the intrinsic instability of liposomes that hinders their biomedical applications.[18]

Here we present quatsomes (QSs), a new class of exceptionally stable SUVs with sizes smaller than 100 nm, formed by the self-assembly in water of cetyl trimethylammonium bromide (CTAB) and cholesterol in a 1:1 ratio, as effective colloidal nanostructures for loading lipophilic and water-insoluble organic dyes resulting in highly stable and bright FONs.[19] Dye-loaded QSs can be prepared by a one-step method using compressed CO_2, named depressurization of expanded liquid organic solution-suspension (DELOS-SUSP), showing several

advantages over conventional routes for the preparation of functionalized vesicles. Indeed, it is a green technology leading in a single step to the formation of multifunctional nanovesicles with superior structural homogeneity.[20–22] As dye models, we used lipophilic fluorophores with long alkyl chains, which can be integrated into QS membrane exploiting hydrophobic interactions between the chains of the dyes and the hydrophobic compartment of the double-layer membrane. Specifically, we use three water-insoluble carbocyanine dyes with two 18-carbons aliphatic chains, 1,1′-dioctadecyl-3,3,3′,3′-tetramethyl-indocarbocyanine perchlorate (DiI), 1,1′-dioctadecyl-3,3,3′,3′-tetramethyl-indodicarbocyanine perchlorate (DiD), and 1,1′-dioctadecyl-3,3,3′,3′-tetramethylindotricarbocyanine iodide (DiR) (**Figure 1**).[23,24] Our experimental results are supported by molecular dynamics (MD) simulations which gave information on the configuration of the dyes within the membrane, and we finally explore the potential of the dye-loaded QSs for biological imaging using dye-loaded QSs as probes for stochastic optical reconstruction microscopy (STORM), an innovative superresolution microscopy technique.[25]

DiD-loaded QSs with DID loadings, L = $\text{moles}_{\text{DID}}$/($\text{moles}_{\text{CTAB}}$ + $\text{moles}_{\text{Cholesterol}}$), ranging from 0.6×10^{-3} to 6.6×10^{-3} (Table S1, Supporting Information) were prepared using the DELOS-SUSP methodology.[21] The physicochemical properties of the resulting vesicles with $L = 1.3 \times 10^{-3}$ (D-QS-2) are here compared with those of other DiD-loaded QSs obtained by other methods generally used for the preparation of loaded vesicles, such as incubation (D-QS-2-IC),[26] sonication (D-QS-2-SON),[19] and thin-film hydration (D-QS-2-TFH).[27] The normalized UV–vis absorption spectra of DiD-loaded QSs prepared by different routes are shown in Figure 1 for comparison along with the spectra of solvated DiD in ethanol (EtOH) and nanoparticles of pure DiD (D-NP) in water, obtained by the DELOS-SUSP method but without using the surfactant (see the Supporting Information). Absorption spectra of DiD-loaded QSs obtained by DELOS-SUSP (D-QS-2) and by thin film hydration (D-QS-2-THF) are very similar to the spectra of solvated DiD in EtOH, showing a narrow band with well-resolved vibronic structure. All other samples show broad spectra with the appearance of intense features on the blue wing of the band, pointing to the formation of H-aggregates,[23,24,28] in line with the well-known tendency of cyanines to aggregate.[28–30] The similarity of spectra of DiD-loaded QSs prepared by DELOS-SUSP and TFH methods suggests that the dye molecules are well dispersed as isolated species inside the QS membrane. However, as shown in CryoTEM images (Figure S2, Supporting Information), D-QS-2 vesicles are much more homogeneous in terms of size and lamellarity than D-QS-2-TFH. DiD-loaded QSs showed several advantages over other DiD-based FONs, such as D-NP and DiD-loaded CTAB micelles (D-MIC), in terms of both optical and colloidal properties. DiD-loaded QSs are colloidally stable during months, with no appreciable changes in size distributions (Table S1, Supporting Information), neither in absorption nor in emission spectra over a 2 month period (**Figure 2**A). On the other hand, the absorption of D-NP decreases steadily following the aggregation of the nanoparticles (Figure S3, Supporting Information). Figure 2B compares visible absorption and emission spectra of D-QS-2 and D-NP. The luminescence of D-NP is completely quenched, in line with the formation of H-aggregates, while the fluorescence spectrum of D-QS-2 is very similar in shape to that of solvated DiD in EtOH. The stability upon dilution of D-QS-2 and D-MIC is compared in Figure S4 (Supporting Information). D-QS-2 maintains its fluorescence at different dilutions, while fluorescence of D-MIC is lower at the same dye concentration and it is quenched at concentrations below the critical micellar concentration of CTAB, suggesting the rupture of micelles and the formation of nonfluorescent DiD aggregates in water.

The effect of dye loading on the physicochemical properties of DiD-loaded QSs was also studied by comparing five different samples with increasing fluorophore loadings with $L = 0.6 \times 10^{-3}$ –6.6×10^{-3} prepared by DELOS-SUSP. Samples are listed in Table S2 (Supporting Information) along with mean size values, measured by nanoparticle tracking analysis. Mean diameters and CryoTEM images (Figure S5, Supporting

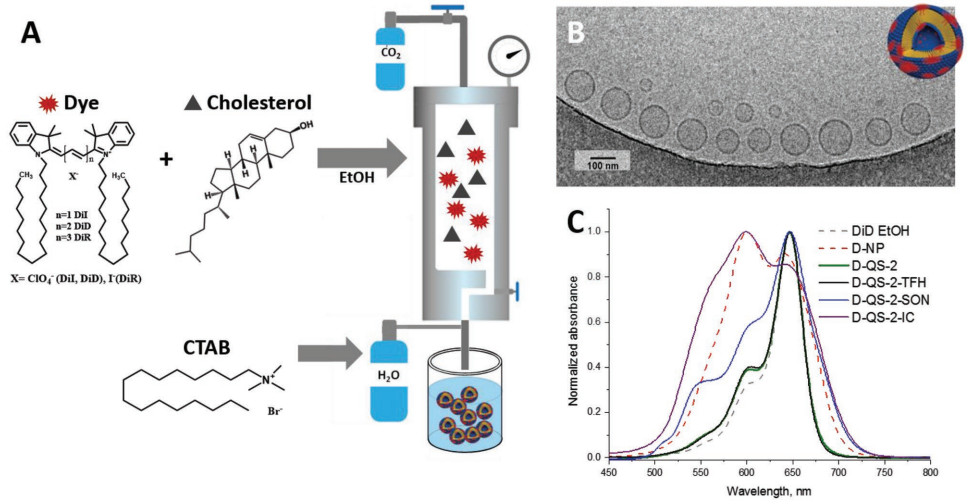

Figure 1. A) Schematic representation of the DELOS-SUSP method for the preparation of QSs loaded with dyes (DiI, DiD, and DiR). B) CryoTEM image of D-QS-2 and C) absorption spectra of DiD in EtOH, DiD-based NPs, and D-QS prepared by different methods (see the text).

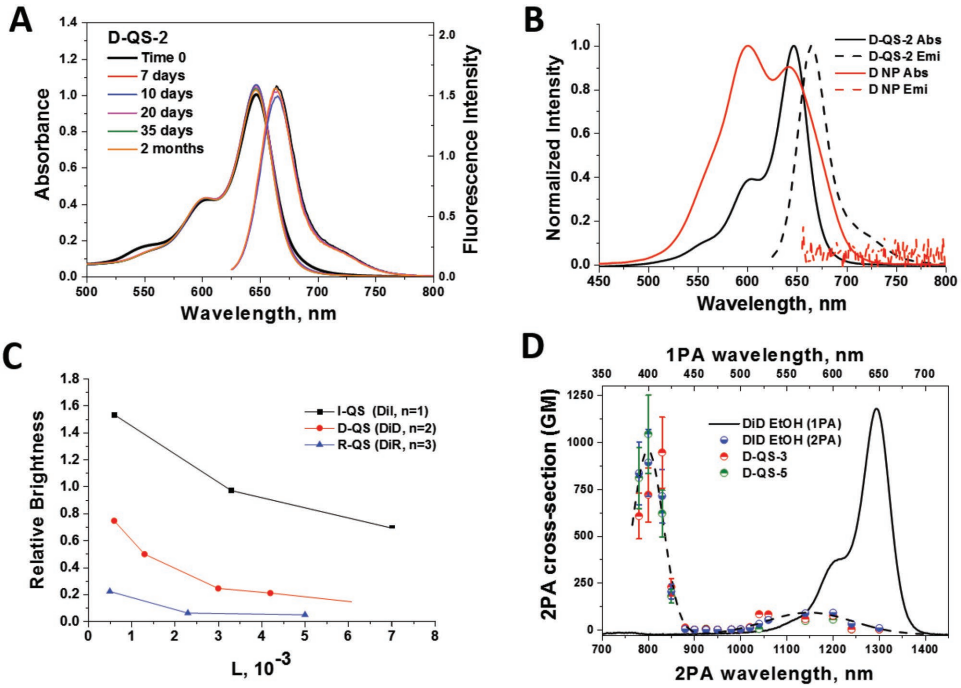

Figure 2. A) Stability of the D-QS-2 sample in water evaluated by UV–vis absorption and emission spectra (λ_{exc} = 610 nm) monitored over 2 months. B) Normalized UV–vis absorption and emission spectra of D-QS-2 and D-NP. C) Relative brightness ($Brightness_{sample}/Brightness_{dye(EtOH)}$) versus loading of the different cyanines-loaded QSs. d) One- (solid line) and two-photon (blue circles) spectra of DiD in EtOH and two-photon spectra of D-QS-3 (red circles) and D-QS-5 (green circles). The dashed line with the shape of the 2PA spectra is shown as guide to the eye.

Information) show that *L* does not affect the vesicle size and morphology. Corresponding absorption spectra in Figure S6A (Supporting Information) show an increase of the intensity on the blue wing of the absorption band, suggesting the progressive formation of nonluminescent H-aggregates in the QS membrane upon increasing the dye concentration, as confirmed by excitation spectra (Figure S6B, Supporting Information) whose shape does not change with the dye loading. The progressive formation of H-aggregates in DiD-loaded QSs with increasing dye loading also explains the decrease of the extinction coefficient (ε) (by a factor of ≈1.8) and of the fluorescence quantum yield (FQY, from 23% to 7%) (Table S2, Supporting Information). The marginal loss of FQY in going from solvated DiD in EtOH (31%) to D-QS-1 (23%) can be ascribed either to the formation of a very small amount of aggregates and/or to environmental effects.[24]

DiI- and DiR-loaded QSs (I-QS and R-QS, respectively in Table S1 in the Supporting Information) were also prepared by the DELOS method with different loadings to study how the length of the conjugated bridge of carbocyanines, *n*, affects the dye aggregation inside the bilayer. Much as for DiD-loaded QSs, the increments in absorbance in the blue wing of R-QS samples point at the formation of H-aggregates (Figure S7B, Supporting Information). On the contrary, the absorption and excitation spectra of I-QS do not support the formation of DiI aggregates in the membrane (Figure S7A, Supporting Information). Overall, the length of the conjugated chain (*n*) of carbocyanines strongly affects the brightness ($\varepsilon \times$ FQY) of fluorescent QSs (Figure 2C). In the case of the shortest chain (DiI), nanostructuration over QSs results in higher brightness compared to the dye in EtOH (up to 50% higher), and high values are maintained even at the highest explored loading (Table S3, Supporting Information). On the contrary, when loaded with DiD and DiR, the formation of nonfluorescent aggregates determines a rapid decrease of the FONs' brightness. Thus, cyanines with longer conjugated structures experience stronger π–π interactions upon nanostructuration, as observed in previous works where cyanines with different polymethine chain sizes were intercalated into DNA strands.[31]

Photostability of DiD in EtOH and of DiD-loaded QSs in water was analyzed by monitoring the evolution over time of the absorbance under continuous laser irradiation (Figure S9, Supporting Information). Relevant photodecomposition quantum yields, determined according to the Belfield method,[32] were obtained (see Table S2 in the Supporting Information). DiD-loaded QSs at any of the assayed loadings are more photostable (≈2 orders of magnitude) than micelle-based nanoformulation of the same dye in water,[33] likely due to the lower photostability of dyes' aggregates,[34,35] which are more in number in the micelles than in QSs. However, DiD-loaded QSs were found less photostable compared to the solvated DiD in EtOH and to its hydrophilic analog Cy5 dissolved in water.

Two-photon absorption (2PA) spectra of DiD in EtOH, and of D-QS-3 and D-QS-5 in water, are shown in Figure 2D. 2PA bandshapes are in agreement with previous works in literature on cyanine dyes.[36] Indeed, DiD in EtOH and DiD-loaded QSs in water show a really narrow main 2PA band, as generally known for cyanines, with values of 2PA cross section around 900 GM. Interestingly, no variations of 2PA bandshapes or of cross sections were found upon increasing the loading of DiD

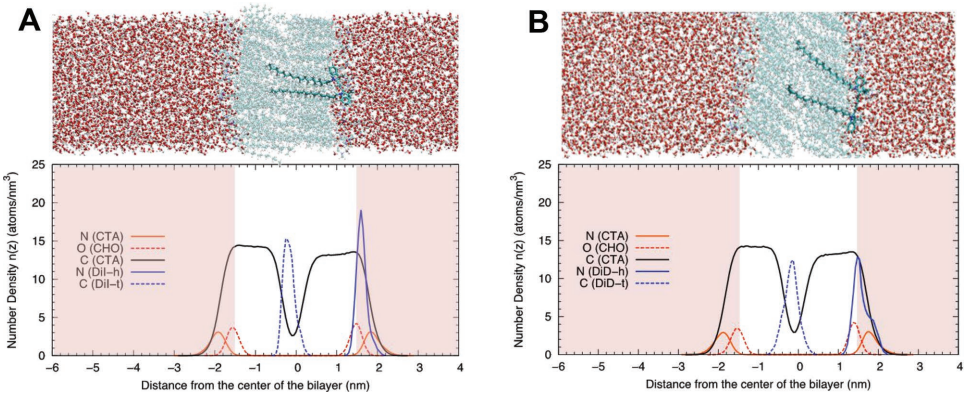

Figure 3. Results from MD simulations for hydrophobic dyes in QSs: A) DiI and B) DiD. For each dye, we show a representative snapshot and the average atomic density profiles of selected atoms in the direction perpendicular to the QS bilayer. In the snapshots, CTAB molecules, water molecules, and the dye molecule (emphasized) are shown in CPK representation. Cholesterol molecules and ions are not shown for clarity. The atomic density profiles indicate the location of two characteristic dye atoms (N from the carbocyanines and terminal C from the alkyl chain), the location of the hydrophobic core (C atoms from CTAB), and the hydrophilic head group region (defined by oxygen atoms from cholesterol —OH and nitrogen atoms from CTAB). The atomic density for dye atoms is multiplied by 100 to help identification of the peaks. The region occupied with water is indicated with a shadow to help interpretation of atomic density profiles. The snapshots and density profiles were made using VMD.[39,40]

in QSs or changing the solvent, confirming that there is no major effect of solvent polarity either on the aggregation state of the dye or on 2PA cross section when DiD is loaded into QSs.

We have employed the NAMD software to perform large-scale MD simulations of DiI- and DiD-loaded QSs in water in order to obtain an atomistic picture of the incorporation of these dyes in QS.[37] Due to the large number of atoms involved in the simulations (10^4–10^5) and the long timescales required (>200 ns), we considered only a QS patch with a single dye molecule (DiI or DiD) in water (all technical details of the MD simulations are summarized in the Supporting Information). In **Figure 3**, we show snapshots from the simulations and the average atomic density profiles. Both DiD and DiI have their carbocyanine groups in contact with water, with their nitrogen atoms located in the hydrophilic region of the QS bilayer (i.e., inside the QS region delimited by the head groups of the CTAB surfactants and the —OH groups of the cholesterol). The carbocyanine groups are on average parallel to the interface for DiD and almost parallel with a small angle of ≈2° for DiI (Figure S11). During the simulations we found configurations with one of the two quinoline groups of each carbocyanine located closer to the membrane interior than the other one (which is closer to water). The aliphatic chains in both carbocyanines are immersed inside the hydrophobic layer of the QS, as expected. As shown in Figure 3, the presence of a dye affects the two leaflets of the QS bilayer. The distance between the density peaks corresponding to carbocyanine nitrogen atoms and the terminal carbon atom of the aliphatic chains is about ≈1.8 nm, compared with the ≈3.4 nm size of the hydrophobic layer of the QS. For both dyes we observe a substantial mobility in the QSs with a motion that can be described as a 2D Brownian motion (see Supporting Information for details), as corresponds to ordinary lateral diffusion over the membrane. We obtain a diffusion coefficient of $D = 4 \times 10^{-11}$ m^2 s^{-1} for DiD and $D = 3.2 \times 10^{-11}$ m^2 s^{-1} for DiI of a similar magnitude to that of phospholipid molecules in a lipid bilayer.[38]

Having extensively characterized promising fluorescent properties of cyanine-loaded QSs, we then explored their potential for imaging. In particular, we demonstrated that thanks to their colloidal and photochemical stability and to the photophysical properties of the loaded dye QSs can be used as probes for STORM superresolution microscopy. STORM is an emerging superresolution technique for biology[25] and nanobiotechnology[41,42] allowing multicolor imaging in vitro or in cells with nanometric resolution.

Figure 4A shows in vitro STORM imaging of DiI-loaded QSs (I-QS-1 sample). DiI photophysical properties inside QSs are suitable for STORM, i.e., they display bright single molecule blinking upon irradiation, allowing accurate molecule localization and reconstruction of superresolved images (Figure 4A, right). DiI distribution appears to be homogeneous inside spherical vesicles with subdiffraction size, in agreement with TEM imaging and spectroscopic characterization (shown in Figures S7A and S8 in the Supporting Information). The images have been quantified to extrapolate the average number of dye localizations and the size of the labeled QSs (Figure 4B). STORM quantification showed an average size of QSs around 99 nm with a relatively narrow distribution (very few QSs are larger than 200 nm) in agreement with CryoTEM results. The localization histogram shows that a large number of DiI molecules is incorporated in the vesicles (mean value of 193 molecular localizations per QS), demonstrating the ability of our formulation to nanostructure a controlled number of dyes into a small vesicle size. The direct visualization and the determination of the exact position in a living biological environment are key aspects of imaging and theranostic agents. For this purpose, DiI-loaded QSs (I-QS-1, diluted at 20×10^{-6} M CTAB concentration) have been incubated with HeLa cells, and live cells' intracellular trafficking has been monitored for 1.5 h using fluorescence microscopy. Figure 4C shows a snapshot of the video (see Figures S12 and S13) after 1 h of incubation. QSs are initially bound to the cellular membrane and subsequently trafficked into cell. This behavior is completely different when only DiI dye is used at the same concentration

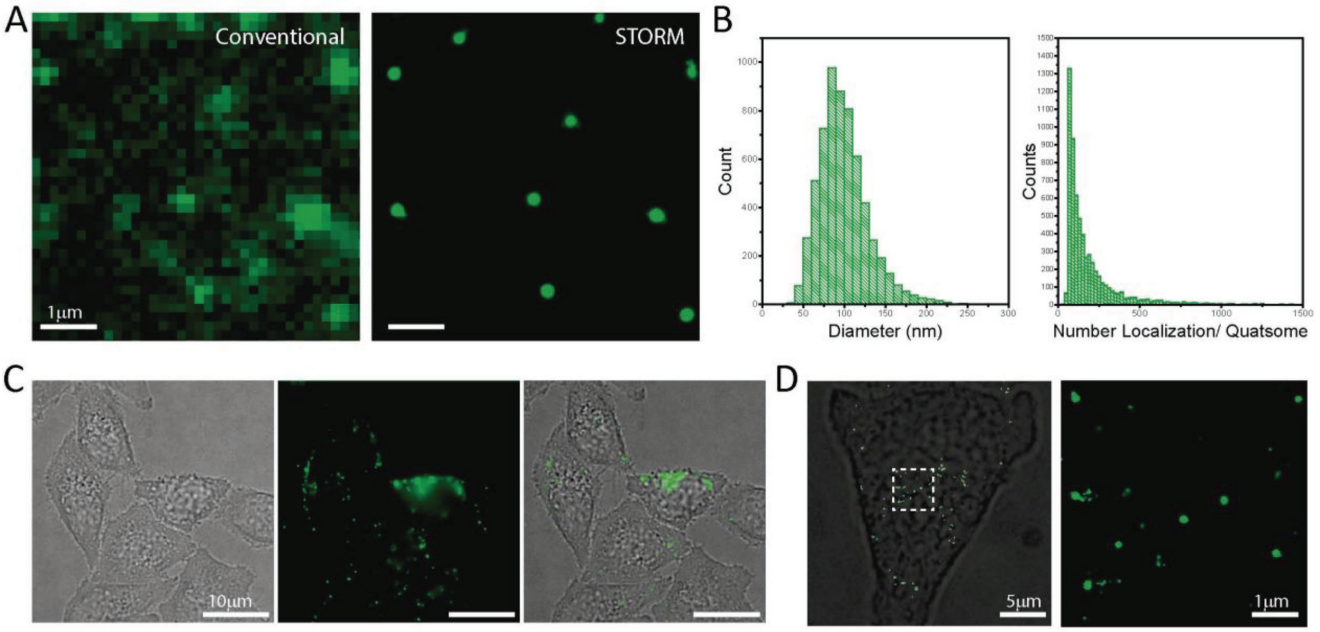

Figure 4. A) Images of DiI-loaded QSs (I-QS-1) obtained by conventional wide-field microscopy and STORM (λ_{exc} = 561 nm). B) Distribution of size and number of localizations per QSs extrapolated from STORM images. C) Snapshot of the video (see the Supporting Information) acquired by fluorescence microscopy of the internalization of QSs in HeLa cells. D) STORM images of QSs internalized in HeLa cells.

since no cell staining was observed (see Figure S10 in the Supporting Information). When using DiI-loaded QSs, after its administration, cells were fixed and the internalized vesicles were visualized by STORM, as shown in Figure 4D. The size of the individually resolved QSs indicates that the vesicles did not undergo aggregation after internalization in cells in agreement with the in vitro studies. Moreover, these measurements show that QSs are still assembled inside cells indicating that their high colloidal stability allows for cellular imaging applications. These measurements show that the size, colloidal stability, and photophysical properties of dye-loaded QSs make them remarkable candidates as nanostructured probes for biological imaging. These results together with the capability of QSs to integrate/encapsulate small drugs or large biomolecules and to decorate their surfaces with targeting groups[21] open the possibility of producing in the near-future multifunctional vesicles for theranostic applications.

Supporting Information

Supporting Information is available from the Wiley Online Library or from the author.

Acknowledgements

This work was financially supported by MINECO/FEDER, Spain (Grant Nos. CTQ2013-40480-R, SAF2016-7524-R, and MAT 2016-80826-R), by AGAUR, Generalitat de Catalunya (Grant No. 2014-SGR-17), and through the CERCA program, the Networking Research Center on Bioengineering, Biomaterials, and Nanomedicine (CIBER-BBN) and the Spanish Ministry of Economy and Competitiveness, through the "Severo Ochoa" Programme for Centres of Excellence in R&D (SEV-2015-0496, Grant FLOWERS, and SEV-2014-0425). L.A. thanks the financial support of AXA Research Fund and D.H. and E.V.S. the Army Research Laboratory (Grant No. W911NF-15-2-0090). The research leading to these results received funding from the People Programme (Marie Curie Actions) of the European Union's Seventh Framework ProgrammeFP7/2007–2013 under REA grant Agreement No. 607721 (Nano2Fun) A.A. and S.I.-T. are enrolled in the Materials Science Ph.D. program of UAB. A.A. and S.I.-T. gratefully acknowledge help of Dr. M. Masino in photostability measurements.

Conflict of Interest

The authors declare no conflict of interest.

Keywords

dyes, fluorescent nanoparticles, molecular dynamics, STORM, vesicles

Received: November 5, 2017
Revised: January 17, 2018
Published online: March 24, 2018

[1] U. Resch-Genger, M. Grabolle, S. Cavaliere-Jaricot, R. Nitschke, T. Nann, *Nat. Methods* **2008**, *5*, 763.
[2] J. W. Lichtman, J.-A. Conchello, *Nat. Methods* **2005**, *2*, 910.
[3] S. Luo, E. Zhang, Y. Su, T. Cheng, C. Shi, *Biomaterials* **2011**, *32*, 7127.
[4] Q. Li, L. Liu, J. W. Liu, J. H. Jiang, R. Q. Yu, X. Chu, *TrAC, Trends Anal. Chem.* **2014**, *58*, 130.

[5] J. Zhang, R. Chen, Z. Zhu, C. Adachi, X. Zhang, C.-S. Lee, *ACS Appl. Mater. Interfaces* **2015**, *7*, 26266.
[6] J. Mérian, J. Gravier, F. Navarro, I. Texier, *Molecules* **2012**, *17*, 5564.
[7] J. Schill, A. P. H. J. Schenning, L. Brunsveld, *Macromol. Rapid Commun.* **2015**, *36*, 1306.
[8] A. Reisch, A. S. Klymchenko, *Small* **2016**, *12*, 1968.
[9] V. Parthasarathy, S. Fery-Forgues, E. Campioli, G. Recher, F. Terenziani, M. Blanchard-Desce, *Small* **2011**, *7*, 3219.
[10] J. U. Menon, P. Jadeja, P. Tambe, K. Vu, B. Yuan, K. T. Nguyen, *Theranostics* **2013**, *3*, 152.
[11] L. Sercombe, T. Veerati, F. Moheimani, S. Y. Wu, A. K. Sood, S. Hua, *Front. Pharmacol.* **2015**, *6*, 1.
[12] S. Li, B. Goins, L. Zhang, A. Bao, *Bioconjugate Chem.* **2012**, *23*, 1322.
[13] V. P. Torchilin, *Nat. Rev. Drug Discovery* **2005**, *4*, 145.
[14] "Reflection paper on the data requirements for intravenous liposomal products developed with reference to an innovator liposomal product"; Committee for Human Medicinal Products, European Medicine Agency, EMA/CHMP/806058/2009/Rev. 02; 13 March 2013, http://www.ema.europa.eu/ema/index.jsp?curl=pages/regulation/general/general_content_000564.jsp&mid=WC0b01ac05806403e0.
[15] X. Wang, E. J. Danoff, N. a. Sinkov, J. H. Lee, S. R. Raghavao, D. S. English, *Langmuir* **2006**, *22*, 6461.
[16] M. Toprak, B. Meryem Aydn, M. Ark, Y. Onganer, *J. Lumin.* **2011**, *131*, 2286.
[17] V. Deissler, R. Rüger, W. Frank, A. Fahr, W. A. Kaiser, I. Hilger, *Small* **2008**, *4*, 1240.
[18] N. Grimaldi, F. Andrade, N. Segovia, L. Ferrer-Tasies, S. Sala, J. Veciana, N. Ventosa, *Chem. Soc. Rev.* **2016**, *45*, 6520.
[19] L. Ferrer-Tasies, E. Moreno-Calvo, M. Cano-Sarabia, M. Aguilella-Arzo, A. Angelova, S. Lesieur, S. Ricart, J. Faraudo, N. Ventosa, J. Veciana, *Langmuir* **2013**, *29*, 6519.
[20] E. Elizondo, J. Larsen, N. S. Hatzakis, I. Cabrera, T. Bjørnholm, J. Veciana, D. Stamou, N. Ventosa, *J. Am. Chem. Soc.* **2012**, *134*, 1918.
[21] I. Cabrera, E. Elizondo, O. Esteban, J. L. Corchero, M. Melgarejo, D. Pulido, A. Córdoba, E. Moreno, U. Unzueta, E. Vazquez, I. Abasolo, S. Schwartz, A. Villaverde, F. Albericio, M. Royo, M. F. García-Parajo, N. Ventosa, J. Veciana, *Nano Lett.* **2013**, *13*, 3766.
[22] E. Elizondo, J. Veciana, N. Ventosa, *Nanomedicine* **2012**, *7*, 1391.
[23] I. Texier, M. Goutayer, A. Da Silva, L. Guyon, N. Djaker, V. Josserand, E. Neumann, J. Bibette, F. Vinet, *J. Biomed. Opt.* **2009**, *14*, 054005.
[24] A. Wagh, S. Y. Qian, B. Law, *Bioconjugate Chem.* **2012**, *23*, 981.
[25] X. Zhuang, *Nat. Photonics* **2009**, *3*, 365.
[26] A. M. Vinogradov, A. S. Tatikolovab, S. M. B. Costa, *Phys. Chem. Chem. Phys.* **2001**, *3*, 4325.
[27] J. S. Dua, A. C. Rana, A. K. Bhandari, *Int. J. Pharm. Stud. Res.* **2012**, *3*, 14.
[28] S. Gadde, E. K. Batchelor, A. E. Kaifer, *Chem. - Eur. J.* **2009**, *15*, 6025.
[29] A. Mishra, R. K. Behera, P. K. Behera, B. K. Mishra, G. B. Behera, *Chem. Rev.* **2000**, *100*, 1973.
[30] G. B. Behera, P. K. Behera, B. K. Mishra, *J. Surf. Sci. Technol.* **2007**, *23*, 1.
[31] Y. Kawabe, S. Kato, *Dyes Pigm.* **2012**, *95*, 614.
[32] C. C. Corredor, K. D. Belfield, M. V. Bondar, O. V. Przhonska, S. Yao, *J. Photochem. Photobiol., A* **2006**, *184*, 105.
[33] H.-Y. Ahn, S. Yao, X. Wang, K. D. Belfield, *ACS Appl. Mater. Interfaces* **2012**, *4*, 2847.
[34] G. V. Zakharova, A. K. Chibisov, *Khim. Vys. Energ.* **2009**, *43*, 346.
[35] M. M. S. Abdel-mottaleb, M. van Der Auweraer, M. S. A. Abdel-mottaleb, *Int. J. Photoenergy* **2004**, *6*, 29.
[36] J. Fu, L. a. Padilha, D. J. Hagan, E. W. Van Stryland, O. V. Przhonska, M. V. Bondar, Y. L. Slominsky, A. D. Kachkovski, *J. Opt. Soc. Am. B* **2007**, *24*, 56.
[37] J. C. Phillips, R. Braun, W. Wang, J. Gumbart, E. Tajkhorshid, E. Villa, C. Chipot, R. D. Skeel, L. Kalé, K. Schulten, *J. Comput. Chem.* **2005**, *26*, 1781.
[38] P. F. F. Almeida, W. L. C. Vaz, in *Handbook of Biological Physics* (Eds: R. Lipowsky, E. Sackmann), Elsevier Science, Amsterdam **1995**, pp. 367–373.
[39] W. Humphrey, A. Dalke, K. Schulten, *J. Mol. Graphics* **1996**, *14*, 33.
[40] T. Giorgino, *Comput. Phys. Commun.* **2014**, *185*, 317.
[41] D. Van Der Zwaag, N. Vanparijs, S. Wijnands, R. De Rycke, B. G. De Geest, L. Albertazzi, *ACS Appl. Mater. Interfaces* **2016**, *8*, 6391.
[42] L. Albertazzi, R. W. Van Der Hofstad, E. W. Meijer, *Science* **2014**, *491*, 10.